Contents

List of Tables

List of Figures

Chapter 6

Classical Interacting Systems

6.1 References

– M. Kardar, *Statistical Physics of Particles* (Cambridge, 2007)
A superb modern text, with many insightful presentations of key concepts.

– L. E. Reichl, *A Modern Course in Statistical Physics* (2nd edition, Wiley, 1998)
A comprehensive graduate level text with an emphasis on nonequilibrium phenomena.

– M. Plischke and B. Bergersen, *Equilibrium Statistical Physics* (3^{rd} edition, World Scientific, 2006)
An excellent graduate level text. Less insightful than Kardar but still a good modern treatment of the subject. Good discussion of mean field theory.

– E. M. Lifshitz and L. P. Pitaevskii, *Statistical Physics* (part I, 3^{rd} edition, Pergamon, 1980)
This is volume 5 in the famous Landau and Lifshitz *Course of Theoretical Physics*. Though dated, it still contains a wealth of information and physical insight.

– J.-P Hansen and I. R. McDonald, *Theory of Simple Liquids* (Academic Press, 1990)
An advanced, detailed discussion of liquid state physics.

6.2 Nonideal Classical Gases

Let's switch gears now and return to the study of continuous classical systems described by a Hamiltonian $\hat{H}\big(\{\boldsymbol{x}_i\},\{\boldsymbol{p}_i\}\big)$. In the next chapter, we will see how the critical properties of classical fluids can in fact be modeled by an appropriate *lattice gas* Ising model, and we'll derive methods for describing the liquid-gas phase transition in such a model.

6.2.1 The configuration integral

Consider the ordinary canonical partition function for a nonideal system of identical point particles interacting via a central two-body potential $u(r)$. We work in the ordinary canonical ensemble. The N-particle partition function is

$$\begin{aligned} Z(T,V,N) &= \frac{1}{N!}\int\prod_{i=1}^{N}\frac{d^d\!p_i\,d^d\!x_i}{h^d}\,e^{-\hat{H}/k_{\rm B}T} \\ &= \frac{\lambda_T^{-Nd}}{N!}\int\prod_{i=1}^{N}d^d\!x_i\,\exp\bigg(-\frac{1}{k_{\rm B}T}\sum_{i<j}u\big(|\boldsymbol{x}_i-\boldsymbol{x}_j|\big)\bigg) \quad . \end{aligned} \tag{6.1}$$

Here, we have assumed a many body Hamiltonian of the form

$$\hat{H}=\sum_{i=1}^{N}\frac{\boldsymbol{p}_i^2}{2m}+\sum_{i<j}u\big(|\boldsymbol{x}_i-\boldsymbol{x}_j|\big) \quad , \tag{6.2}$$

in which massive nonrelativistic particles interact via a two-body central potential. As before, $\lambda_T=\sqrt{2\pi\hbar^2/mk_{\rm B}T}$ is the thermal wavelength. We can now write

$$Z(T,V,N)=\lambda_T^{-Nd}\,Q_N(T,V) \quad , \tag{6.3}$$

where the *configuration integral* $Q_N(T,V)$ is given by

$$Q_N(T,V)=\frac{1}{N!}\int\!d^d\!x_1\cdots\int\!d^d\!x_N\,\prod_{i<j}e^{-\beta u(r_{ij})} \quad . \tag{6.4}$$

There are no general methods for evaluating the configurational integral exactly.

6.2.2 One-dimensional Tonks gas

The Tonks gas is a one-dimensional generalization of the hard sphere gas. Consider a one-dimensional gas of indistinguishable particles of mass m interacting via the potential

$$u(x-x')=\begin{cases}\infty & \text{if } |x-x'|<a \\ 0 & \text{if } |x-x'|\geq a \quad .\end{cases} \tag{6.5}$$

Thus, the Tonks gas may be considered to be a gas of *hard rods*. The above potential guarantees that the portion of configuration space in which any rods overlap is *forbidden* in this model. Let the gas be placed in a finite volume L. The hard sphere nature of the particles means that no particle can get within a distance $\frac{1}{2}a$ of the ends at $x = 0$ and $x = L$. That is, there is a one-body potential $v(x)$ acting as well, where

$$v(x) = \begin{cases} \infty & \text{if } x < \frac{1}{2}a \\ 0 & \text{if } \frac{1}{2}a \le x \le L - \frac{1}{2}a \\ \infty & \text{if } x > L - \frac{1}{2}a \quad . \end{cases} \tag{6.6}$$

The configuration integral of the 1D Tonks gas is given by

$$Q_N(T,L) = \frac{1}{N!} \int\limits_0^L dx_1 \cdots \int\limits_0^L dx_N \, \chi(x_1, \ldots, x_N) \quad , \tag{6.7}$$

where $\chi = e^{-U/k_\text{B}T}$ is zero if any two 'rods' (of length a) overlap, or if any rod overlaps with either boundary at $x = 0$ and $x = L$, and $\chi = 1$ otherwise. Note that χ does not depend on the temperature. Due to permutation symmetry, we may integrate over the subspace where $x_1 < x_2 < \cdots < x_N$ and then multiply the result by $N!$. Clearly x_j must lie to the right of $x_{j-1} + a$ as well as to the left of $Y_j \equiv L - Na + (j - \frac{1}{2})a$. Note that since $Y_j - a = Y_{j-1}$. Thus, the configurational integral is

$$\begin{aligned} Q_N(T,L) &= \int\limits_{a/2}^{Y_1} dx_1 \int\limits_{x_1+a}^{Y_2} dx_2 \cdots \int\limits_{x_{N-1}+a}^{Y_N} dx_N = \int\limits_{a/2}^{Y_1} dx_1 \int\limits_{x_1+a}^{Y_2} dx_2 \cdots \int\limits_{x_{N-2}+a}^{Y_{N-1}} dx_{N-1} \, \big(Y_{N-1} - x_{N-1}\big) \\ &= \frac{1}{2} \int\limits_{a/2}^{Y_1} dx_1 \int\limits_{x_1+a}^{Y_2} dx_2 \cdots \int\limits_{x_{N-3}+a}^{Y_{N-2}} dx_{N-2} \, \big(Y_{N-2} - x_{N-2}\big)^2 = \cdots = \frac{1}{k!} \int\limits_{a/2}^{Y_1} dx_1 \int\limits_{x_1+a}^{Y_2} dx_2 \cdots \int\limits_{x_{N-k-1}+a}^{Y_{N-k}} dx_{N-k} \, \big(Y_{N-k} - x_{N-k}\big)^k \\ &= \frac{1}{N!} \big(Y_1 - \tfrac{1}{2}a\big)^N = \frac{1}{N!} \, (L - Na)^N \quad . \end{aligned} \tag{6.8}$$

The partition function is $Z(T,L,N) = \lambda_T^{-N} \, Q_N(T,L)$, and so the free energy is

$$F = -k_\text{B}T \log Z = -Nk_\text{B}T \left\{ -\log \lambda_T + 1 + \log\left(\frac{L}{N} - a\right) \right\} \quad , \tag{6.9}$$

where we have used Stirling's rule to write $\log N! \approx N \log N - N$. The pressure is

$$p = -\frac{\partial F}{\partial L} = \frac{nk_\text{B}T}{1 - na} \quad , \tag{6.10}$$

where $n = N/L$ is the one-dimensional density. Note that the pressure diverges as n approaches $1/a$. The usual one-dimensional ideal gas law, $pL = Nk_\text{B}T$, is replaced by $pL_\text{eff} = Nk_\text{B}T$, where $L_\text{eff} = L - Na$ is the 'free' volume obtained by subtracting the total "excluded volume" Na from the original volume L.

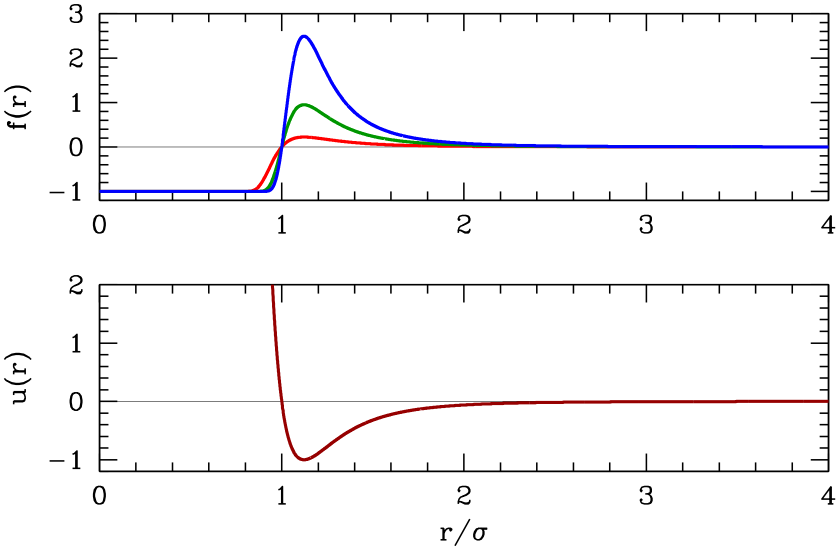

Figure 6.1: Bottom panel: Lennard-Jones potential $u(r) = 4\epsilon\left(x^{-12} - x^{-6}\right)$, with $x = r/\sigma$ and $\epsilon = 1$. Note the weak attractive tail and the strong repulsive core. Top panel: Mayer function $f(r,T) = e^{-u(r)/k_\mathrm{B}T} - 1$ for $k_\mathrm{B}T = 0.8\,\epsilon$ (blue), $k_\mathrm{B}T = 1.5\,\epsilon$ (green), and $k_\mathrm{B}T = 5\,\epsilon$ (red).

Note the similarity here to the van der Waals equation of state, $(p + av^{-2})(v - b) = RT$, where $v = N_\mathrm{A}V/N$ is the molar volume. Defining $\tilde{a} \equiv a/N_\mathrm{A}^2$ and $\tilde{b} \equiv b/N_\mathrm{A}$, we have

$$p + \tilde{a}n^2 = \frac{nk_\mathrm{B}T}{1 - \tilde{b}n} \quad , \tag{6.11}$$

where $n = N_\mathrm{A}/v$ is the number density. The term involving the constant $\tilde{a}$ is due to the long-ranged attraction of atoms due to their mutual polarizability. The term involving $\tilde{b}$ is an excluded volume effect. The Tonks gas models only the latter.

6.2.3 Mayer cluster expansion

Let us return to the general problem of computing the configuration integral. Consider the function $e^{-\beta u_{ij}}$, where $u_{ij} \equiv u(|\boldsymbol{x}_i - \boldsymbol{x}_j|)$. We assume that at very short distances there is a strong repulsion between particles, *i.e.* $u_{ij} \to \infty$ as $r_{ij} = |\boldsymbol{x}_i - \boldsymbol{x}_j| \to 0$, and that $u_{ij} \to 0$ as $r_{ij} \to \infty$. Thus, $e^{-\beta u_{ij}}$ vanishes as $r_{ij} \to 0$ and approaches unity as $r_{ij} \to \infty$. For our purposes, it will prove useful to define the function

$$f(r) = e^{-\beta u(r)} - 1 \quad , \tag{6.12}$$

called the *Mayer function* after Josef Mayer. We may now write

$$Q_N(T,V) = \frac{1}{N!}\int d^d\!x_1 \cdots \int d^d\!x_N \prod_{i<j}\left(1 + f_{ij}\right) \quad . \tag{6.13}$$

A typical potential we might consider is the semi-phenomenological Lennard-Jones potential,

$$u(r) = 4\,\epsilon \left\{ \left(\frac{\sigma}{r}\right)^{12} - \left(\frac{\sigma}{r}\right)^{6} \right\} \quad . \tag{6.14}$$

This accounts for a long-distance attraction due to mutually induced electric dipole fluctuations, and a strong short-ranged repulsion, phenomenologically modelled with a r^{-12} potential, which mimics a hard core due to overlap of the atomic electron distributions. Setting $u'(r) = 0$ we obtain $r^* = 2^{1/6}\,\sigma \approx 1.12246\,\sigma$ at the minimum, where $u(r^*) = -\epsilon$. In contrast to the Boltzmann weight $e^{-\beta u(r)}$, the Mayer function $f(r)$ vanishes as $r \to \infty$, behaving as $f(r) \sim -\beta u(r)$. The Mayer function also depends on temperature. Sketches of $u(r)$ and $f(r)$ for the Lennard-Jones model are shown in fig. 6.1.

The Lennard-Jones potential is realistic for certain simple fluids, but it leads to a configuration integral which is in general impossible to evaluate. Indeed, even a potential as simple as that of the hard sphere gas is intractable in more than one space dimension. We can however make progress by deriving a series expansion for the equation of state in powers of the particle density. This is known as the *virial expansion*. As was the case when we investigated noninteracting quantum statistics, it is convenient to work in the grand canonical ensemble and to derive series expansions for the density $n(T,z)$ and the pressure $p(T,z)$ in terms of the fugacity z, then solve for $z(T,n)$ to obtain $p(T,n)$. These expansions in terms of fugacity have a nifty diagrammatic interpretation, due to Mayer.

We begin by expanding the product in eqn. 6.13 as

$$\prod_{i<j} \big(1 + f_{ij}\big) = 1 + \sum_{i<j} f_{ij} + \sum_{\substack{i<j\,,\,k<l \\ (ij)\neq(kl)}} f_{ij}\, f_{kl} + \ldots \quad . \tag{6.15}$$

As there are $\frac{1}{2}N(N-1)$ possible pairings, there are $2^{N(N-1)/2}$ terms in the expansion of the above product. Each such term may be represented by a graph, as shown in fig. 6.2. For each such term, we draw a connection between dots representing different particles i and j if the factor f_{ij} appears in the term under consideration. The contribution for any given graph may be written as a product over contributions from each of its disconnected component clusters. For example, in the case of the term in fig. 6.2, the contribution to the configurational integral would be

$$\begin{aligned} \Delta Q = \frac{V^{N-11}}{N!} & \int \! d^d\!x_1\, d^d\!x_4\, d^d\!x_7\, d^d\!x_9\; f_{1,4}\, f_{4,7}\, f_{4,9}\, f_{7,9} \\ & \times \int \! d^d\!x_2\, d^d\!x_5\, d^d\!x_6\; f_{2,5}\, f_{2,6} \times \int \! d^d\!x_3\, d^d\!x_{10}\; f_{3,10} \times \int \! d^d\!x_8\, d^d\!x_{11}\; f_{8,11} \quad . \end{aligned} \tag{6.16}$$

We will refer to a given product of Mayer functions which arises from this expansion as a *term*.

The particular labels we assign to each vertex of a given graph don't affect the overall value of the graph. Now a given unlabeled graph consists of a certain number of connected subgraphs. For a system with N particles, we may then write

$$N = \sum_\gamma m_\gamma\, n_\gamma \quad , \tag{6.17}$$

where γ ranges over all possible connected subgraphs, and

$m_\gamma =$ number of connected subgraphs of type γ in the unlabeled graph
$n_\gamma =$ number of vertices in the connected subgraph γ .

$$\big(f_{1,4}\, f_{4,7}\, f_{4,9}\, f_{7,9}\big)\,\big(f_{2,5}\, f_{2,6}\big)\,\big(f_{3,10}\big)\,\big(f_{8,11}\big)$$

$$\Updownarrow$$

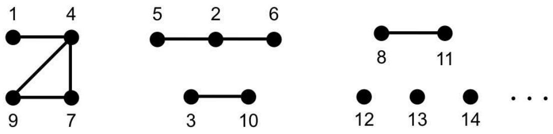

Figure 6.2: Diagrammatic interpretation of a term involving a product of eight Mayer functions.

Note that the single vertex • counts as a connected subgraph, with $n_\bullet = 1$. We now ask: how many ways are there of assigning the N labels to the N vertices of a given unlabeled graph? One might first thing the answer is simply $N!$, however this is too big, because different assignments of the labels to the vertices may not result in a distinct graph. To see this, consider the examples in fig. 6.3. In the first example, an unlabeled graph with four vertices consists of two identical connected subgraphs. Given any assignment of labels to the vertices, then, we can simply exchange the two subgraphs and get the same term. So we should divide $N!$ by the product $\prod_\gamma m_\gamma!$. But even this is not enough, because within each connected subgraph γ there may be permutations which leave the integrand unchanged, as shown in the second and third examples in fig. 6.3. We define the *symmetry factor* s_γ as the number of permutations of the labels which leaves a given connected subgraphs γ invariant. Examples of symmetry factors are shown in fig. 6.4. Consider, for example, the third subgraph in the top row. Clearly one can rotate the figure about its horizontal symmetry axis to obtain a new labeling which represents the same term. This twofold axis is the only symmetry the diagram possesses, hence $s_\gamma = 2$. For the first diagram in the second row, one can rotate *either* of the triangles about the horizontal symmetry axis. One can also rotate the figur e in the plane by 180° so as to exchange the two triangles. Thus, there are $2 \times 2 \times 2 = 8$ symmetry operations which result in the same term, and $s_\gamma = 8$. Finally, the last subgraph in the second row consists of five vertices each of which is connected to the other four. Therefore any permutation of the labels results in the same term, and $s_\gamma = 5! = 120$. In addition to dividing by the product $\prod_\gamma m_\gamma!$, we must then also divide by $\prod_\gamma s_\gamma^{m_\gamma}$.

We can now write the partition function as

$$\begin{aligned} Z &= \frac{\lambda_T^{-Nd}}{N!} \sum_{\{m_\gamma\}} \frac{N!}{\prod m_\gamma!\, s_\gamma^{m_\gamma}} \cdot \prod_\gamma \bigg(\int \! d^d\!x_1 \cdots d^d\!x_{n_\gamma} \prod_{i<j}^{\gamma} f_{ij} \bigg)^{m_\gamma} \delta_{N\,,\sum m_\gamma n_\gamma} \\ &= \sum_{\{m_\gamma\}} \prod_\gamma \frac{1}{m_\gamma!} \bigg(\frac{V b_\gamma(T)}{\lambda_T^d} \bigg)^{m_\gamma} \delta_{N\,,\sum m_\gamma n_\gamma} \end{aligned} \qquad (6.18)$$

where the product $\prod_{i<j}^{\gamma} f_{ij}$ is over all links in the subgraph γ. The final Kronecker delta enforces the constraint $N = \sum_\gamma m_\gamma\, n_\gamma$. We have defined the *dimensionless cluster integrals* b_γ as

$$b_\gamma(T) \equiv \frac{1}{s_\gamma} \int \! \frac{d^d\!x_1}{\lambda_T^d} \cdots \int \! \frac{d^d\!x_{n_\gamma - 1}}{\lambda_T^d} \prod_{i<j}^{\gamma} f_{ij} \quad , \qquad (6.19)$$

where we assume the limit $V \to \infty$. Since $f_{ij} = f\big(|\boldsymbol{x}_i - \boldsymbol{x}_j|\big)$, the product $\prod_{i<j}^{\gamma} f_{ij}$ is invariant under

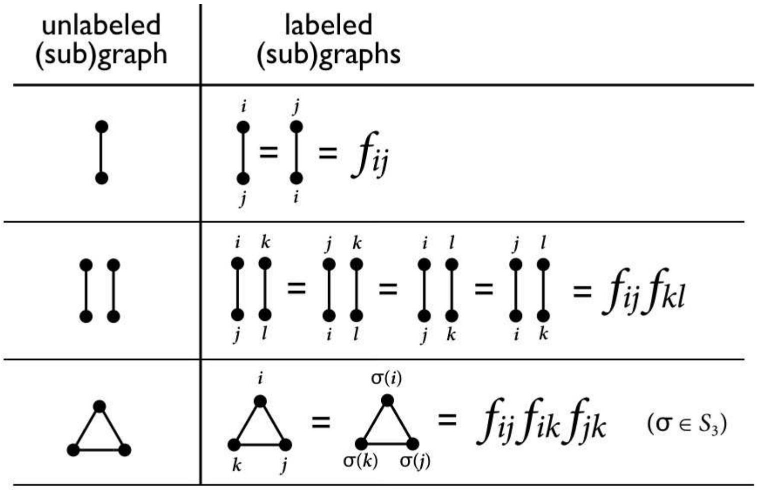

Figure 6.3: Different assignations of labels to vertices may not result in a distinct term in the expansion of the configuration integral.

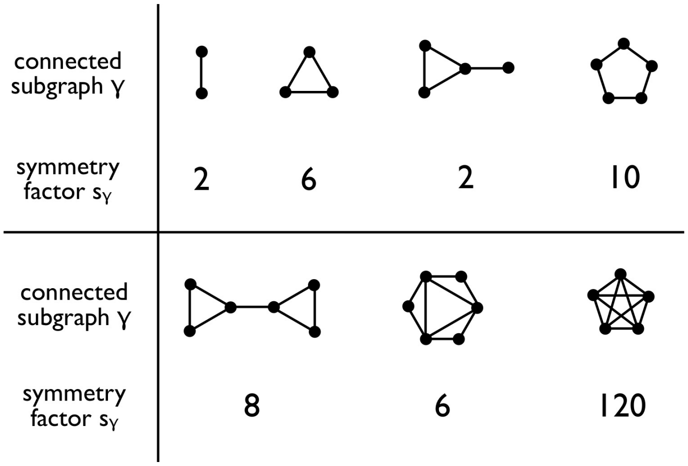

Figure 6.4: The symmetry factor s_γ for a connected subgraph γ is the number of permutations of its indices which leaves the term $\prod_{(ij)\in\gamma} f_{ij}$ invariant.

simultaneous translation of all the coordinate vectors by any constant vector, and hence the integral over the n_γ position variables contains exactly one factor of the volume, which yields factor of V within the round brackets in the second line of eqn. 6.18. Thus, each cluster integral is *intensive*[1], scaling as V^0.

If we compute the grand partition function, then the fixed N constraint is relaxed, and we can do the

---

[1] We assume that the long-ranged behavior of $f(r) \approx -\beta u(r)$ is integrable.

sums:

$$
\begin{aligned}
\mathit{\Xi}(T,V,\mu) &= \sum_{\{m_\gamma\}} \big(e^{\beta\mu}\big)^{\sum m_\gamma n_\gamma} \prod_\gamma \frac{1}{m_\gamma !} \bigg(\frac{V b_\gamma(T)}{\lambda_T^d}\bigg)^{m_\gamma} \\
&= \prod_\gamma \sum_{m_\gamma=0}^{\infty} \frac{1}{m_\gamma !} \bigg(\frac{V z^{n_\gamma}\, b_\gamma(T)}{\lambda_T^d}\bigg)^{m_\gamma} = \exp\bigg(V \lambda_T^{-d} \sum_\gamma z^{n_\gamma}\, b_\gamma\bigg) \quad ,
\end{aligned}
\tag{6.20}
$$

where $z = \exp(\beta\mu)$ is the fugacity. Thus, since $\mathit{\Omega} = -k_{\rm B}T \log \mathit{\Xi}$,

$$
\mathit{\Omega}(T,V,\mu) = -\frac{V k_{\rm B} T}{\lambda_T^d} \sum_\gamma z^{n_\gamma}\, b_\gamma(T) \quad ,
\tag{6.21}
$$

and we can write

$$
\begin{aligned}
p &= k_{\rm B}T\, \lambda_T^{-d} \sum_\gamma z^{n_\gamma}\, b_\gamma(T) \\
n &= \lambda_T^{-d} \sum_\gamma n_\gamma\, z^{n_\gamma}\, b_\gamma(T) \quad ,
\end{aligned}
\tag{6.22}
$$

where $b_\bullet \equiv 1$. As in the case of ideal quantum gas statistical mechanics, we can systematically invert the relation $n = n(z,T)$ to obtain $z = z(n,T)$, and then insert this into the equation for $p(z,T)$ to obtain the equation of state $p = p(n,T)$. This yields the *virial expansion* of the equation of state,

$$
p = n k_{\rm B} T \Big\{ 1 + B_2(T)\, n + B_3(T)\, n^2 + \ldots \Big\} \quad .
\tag{6.23}
$$

Lowest order expansion

We may rather easily obtain

$$
B_2(T) = -\lambda_T^d\, b_-(T) \qquad , \qquad B_3(T) = 2\lambda_T^{2d}\, b_\triangle(T) \quad ,
\tag{6.24}
$$

with

$$
b_-(T) = \tfrac{1}{2}\int \frac{d^d\! x_1}{\lambda_T^d}\, f\big(|\boldsymbol{x}_1 - \boldsymbol{x}_2|\big) = \tfrac{1}{2}\int \frac{d^d\! r}{\lambda_T^d}\, f(r)
\tag{6.25}
$$

and

$$
\begin{aligned}
b_\wedge(T) &= \tfrac{1}{2}\int \frac{d^d\! x_1}{\lambda_T^d} \int \frac{d^d\! x_2}{\lambda_T^d}\, f\big(|\boldsymbol{x}_1 - \boldsymbol{x}_2|\big)\, f\big(|\boldsymbol{x}_1 - \boldsymbol{x}_3|\big) \\
&= \tfrac{1}{2}\int \frac{d^d\! r}{\lambda_T^d} \int \frac{d^d\! r'}{\lambda_T^d}\, f(r)\, f(r') = 2\big(b_-\big)^2
\end{aligned}
\tag{6.26}
$$

and

$$
\begin{aligned}
b_\triangle(T) &= \tfrac{1}{6}\int \frac{d^d\! x_1}{\lambda_T^d} \int \frac{d^d\! x_2}{\lambda_T^d}\, f\big(|\boldsymbol{x}_1 - \boldsymbol{x}_2|\big)\, f\big(|\boldsymbol{x}_1 - \boldsymbol{x}_3|\big)\, f\big(|\boldsymbol{x}_2 - \boldsymbol{x}_3|\big) \\
&= \tfrac{1}{6}\int \frac{d^d\! r}{\lambda_T^d} \int \frac{d^d\! r'}{\lambda_T^d}\, f(r)\, f(r')\, f\big(|\boldsymbol{r} - \boldsymbol{r}'|\big) \quad .
\end{aligned}
\tag{6.27}
$$

Cookbook recipe

Just follow these simple steps:

- The pressure and number density are written as sums over unlabeled connected clusters γ, *viz.*

$$\begin{aligned} p &= k_{\rm B}T\,\lambda_T^{-d}\sum_\gamma z^{n_\gamma}\,b_\gamma(T) \\ n &= \lambda_T^{-d}\sum_\gamma n_\gamma\,z^{n_\gamma}\,b_\gamma(T) \quad , \end{aligned} \tag{6.28}$$

  where $z=\exp(\beta\mu)$ is the fugacity.

- To compute the dimensionless cluster integral $b_\gamma(T)$, first draw the connected cluster γ with *unlabeled* vertices.
- Next, assign labels $1\,,\,2\,,\,\ldots\,,\,n_\gamma$ to the vertices, where n_γ is the total number of vertices in the cluster γ. It doesn't matter how you assign the labels.
- Write down the product $\prod_{i<j}^\gamma f_{ij}$. The factor f_{ij} appears in the product if there is a link in your (now labeled) cluster between sites i and j.
- The symmetry factor s_γ is the number of elements of the symmetric group S_{n_γ} which leave the product $\prod_{i<j}^\gamma f_{ij}$ invariant. The identity permutation leaves the product invariant, so $s_\gamma \geq 1$.
- The dimensionless cluster integral $b_\gamma(T)$ is given by

$$b_\gamma(T) \equiv \frac{1}{s_\gamma}\int\!\frac{d^d\!x_1}{\lambda_T^d}\cdots\int\!\frac{d^d\!x_{n_\gamma-1}}{\lambda_T^d}\prod_{i<j}^\gamma f_{ij} \quad , \tag{6.29}$$

  Due to translation invariance, $b_\gamma(T)\propto V^0$. One can therefore set $\boldsymbol{x}_{n_\gamma}\equiv 0$, eliminate the volume factor from the denominator, and perform the integral over the remaining $n_\gamma - 1$ coordinates.

- This procedure generates expansions for $p(T,z)$ and $n(T,z)$ in powers of the fugacity $z=\exp(\beta\mu)$. To obtain something useful like $p(T,n)$, we mut invert the equation $n=n(T,z)$ to find $z=z(T,n)$, and then substitute into the equation $p=p(T,z)$ to obtain $p=p\big(T,z(T,n)\big)=p(T,n)$. The result is the virial expansion,

$$p = nk_{\rm B}T\,\Big\{1+B_2(T)\,n+B_3(T)\,n^2+\ldots\Big\} \quad , \tag{6.30}$$

  where

$$B_k(T) = -(k-1)\,\lambda_T^{(k-1)d}\sum_{\gamma\in\varGamma_k} b_\gamma(T) \quad , \tag{6.31}$$

  with $\varGamma_k$ the set of all one-particle irreducible (1PI) k-site clusters. A 1PI cluster remains connected if any of its sites and all that site's connecting links are removed.

6.2.4 Examples

Hard sphere gas in three dimensions

The hard sphere potential is given by

$$u(r) = \begin{cases} \infty & \text{if } r \le a \\ 0 & \text{if } r > a \end{cases} \quad . \tag{6.32}$$

Here a is the *diameter* of the spheres. The corresponding Mayer function is then temperature independent, and given by

$$f(r) = \begin{cases} -1 & \text{if } r \le a \\ 0 & \text{if } r > a \end{cases} \quad . \tag{6.33}$$

We can change variables to obtain

$$\mathsf{b}_2(T) = \tfrac{1}{2} \int \frac{d^3\!r}{\lambda_T^3}\, f(r) = -\tfrac{2}{3}\pi a^3 \lambda_T^{-3} \quad . \tag{6.34}$$

The calculation of b_3 is more challenging. We have

$$\mathsf{b}_3 = \tfrac{1}{6} \int \frac{d^3\!\rho}{\lambda_T^3} \int \frac{d^3\!r}{\lambda_T^3}\, f(\rho)\, f(r)\, f\big(|\boldsymbol{r} - \boldsymbol{\rho}|\big) \quad . \tag{6.35}$$

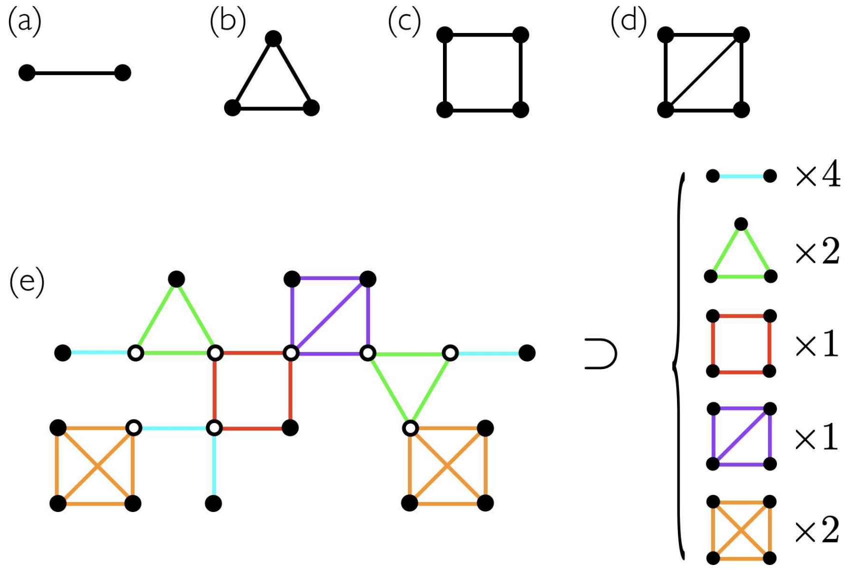

Figure 6.5: Connected *versus* irreducible clusters. Clusters (a) through (d) are *irreducible* in that they remain connected if any component site and its connecting links are removed. Cluster (e) is connected, but is *reducible*. Its integral b_γ is proportional to a product over its irreducible components, each shown in a unique color, and occurring with various multiplicities. The open circles denote *articulation points*. Removal of an articulation point and all the links connected to it results in a disconnected diagram. Removal of any of the closed circles and its associated links does not result in a disconnected diagram.

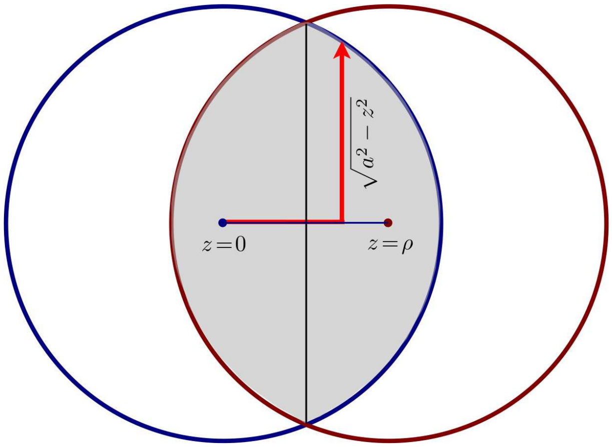

Figure 6.6: The overlap of hard sphere Mayer functions. The shaded volume is $\mathcal{V}$.

We must first compute the volume of overlap for spheres of *radius* a (recall a is the *diameter* of the constituent hard sphere particles) centered at 0 and at $\boldsymbol{\rho}$:

$$\begin{aligned}\mathcal{V} &= \int\! d^3\!r\, f(r)\, f\big(|\boldsymbol{r}-\boldsymbol{\rho}|\big)\\ &= 2\int\limits_{\rho/2}^{a}\! dz\; \pi(a^2-z^2) = \tfrac{4\pi}{3}a^3 - \pi a^2\rho + \tfrac{\pi}{12}\,\rho^3 \quad .\end{aligned} \tag{6.36}$$

We then integrate over region $|\boldsymbol{\rho}| < a$, to obtain

$$\mathsf{b}_3 = -\tfrac{1}{6}\cdot 4\pi\lambda_T^{-6}\int\limits_0^a\! d\rho\,\rho^2 \cdot \Big\{\tfrac{4\pi}{3}a^3 - \pi a^2\rho + \tfrac{\pi}{12}\,\rho^3\Big\} = -\tfrac{5\pi^2}{36}\,a^6\lambda_T^{-6} \quad . \tag{6.37}$$

Thus, we have

$$B_2(T) = -\lambda_T^3\,\mathsf{b}_2(T) = \tfrac{2\pi}{3}a^3 \qquad , \qquad B_3(T) = -2\lambda_T^6\,\mathsf{b}_3(T) = \tfrac{5\pi^2}{18}a^6 \tag{6.38}$$

and the equation of state is then

$$p = nk_{\rm B}T\,\Big\{1 + \tfrac{2\pi}{3}a^3 n + \tfrac{5\pi^2}{18}a^6 n^2 + \mathcal{O}(n^3)\Big\} \quad . \tag{6.39}$$

Weakly attractive tail

Suppose

$$u(r) = \begin{cases} \infty & \text{if } r \le a \\ -u_0(r) & \text{if } r > a \end{cases} \quad . \tag{6.40}$$

Then the corresponding Mayer function is

$$f(r)=\begin{cases}-1 & \text{if } r\le a\\ e^{\beta u_0(r)}-1 & \text{if } r>a\quad .\end{cases}\tag{6.41}$$

Thus,

$$\mathsf{b}_2(T)=\tfrac{1}{2}\int\!\frac{d^3\!r}{\lambda_T^3}\,f(r)=-\tfrac{2\pi}{3}a^3\lambda_T^{-3}+2\pi\lambda_T^{-3}\int\limits_a^\infty\!dr\,r^2\left[e^{\beta u_0(r)}-1\right]\quad .\tag{6.42}$$

Thus, the second virial coefficient is

$$B_2(T)=-\lambda_T^3\,\mathsf{b}_2(T)\approx\tfrac{2\pi}{3}a^3-\frac{2\pi}{k_{\rm B}T}\int\limits_a^\infty\!dr\,r^2\,u_0(r)\quad ,\tag{6.43}$$

where we have assumed $k_{\rm B}T\ll u_0(r)$. We see that the second virial coefficient *changes sign* at some temperature T_0, from a negative low temperature value to a positive high temperature value.

Spherical potential well

Consider an attractive spherical well potential with an infinitely repulsive core,

$$u(r)=\begin{cases}\infty & \text{if } r\le a\\ -\epsilon & \text{if } a<r<R\\ 0 & \text{if } r>R\quad .\end{cases}\tag{6.44}$$

Then the corresponding Mayer function is

$$f(r)=\begin{cases}-1 & \text{if } r\le a\\ e^{\beta\epsilon}-1 & \text{if } a<r<R\\ 0 & \text{if } r>R\quad .\end{cases}\tag{6.45}$$

Writing $s\equiv R/a$, we have

$$\begin{aligned}B_2(T)=-\lambda_T^3\,\mathsf{b}_2(T)&=-\tfrac{1}{2}\int\!d^3\!r\,f(r)\\ &=-\frac{1}{2}\left\{(-1)\cdot\tfrac{4\pi}{3}a^3+\big(e^{\beta\epsilon}-1\big)\cdot\tfrac{4\pi}{3}a^3(s^3-1)\right\}\\ &=\tfrac{2\pi}{3}a^3\left\{1-(s^3-1)\big(e^{\beta\epsilon}-1\big)\right\}\quad .\end{aligned}\tag{6.46}$$

To find the temperature T_0 where $B_2(T)$ changes sign, we set $B_2(T_0)=0$ and obtain

$$k_{\rm B}T_0=\epsilon\Big/\log\!\left(\frac{s^3}{s^3-1}\right)\quad .\tag{6.47}$$

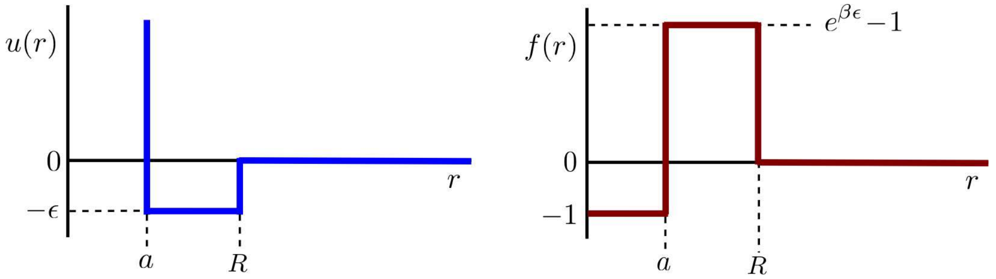

Figure 6.7: An attractive spherical well with a repulsive core $u(r)$ and its associated Mayer function $f(r)$.

Recall in our study of the thermodynamics of the Joule-Thompson effect in §2.10.7 that the throttling process is *isenthalpic*. The temperature change, when a gas is pushed (or escapes) through a porous plug from a high pressure region to a low pressure one is

$$\Delta T = \int_{p_1}^{p_2} dp\, \left(\frac{\partial T}{\partial p}\right)_H \quad , \tag{6.48}$$

where

$$\left(\frac{\partial T}{\partial p}\right)_H = \frac{1}{C_p}\left[T\left(\frac{\partial V}{\partial T}\right)_p - V\right] \quad . \tag{6.49}$$

Appealing to the virial expansion, and working to lowest order in corrections to the ideal gas law, we have

$$p = \frac{N}{V}\,k_{\rm B}T + \frac{N^2}{V^2}\,k_{\rm B}T\,B_2(T) + \ldots \tag{6.50}$$

and we compute $\big(\frac{\partial V}{\partial T}\big)_p$ by setting

$$0 = dp = -\frac{Nk_{\rm B}T}{V^2}\,dV + \frac{Nk_{\rm B}}{V}\,dT - \frac{2N^2}{V^3}\,k_{\rm B}T\,B_2(T)\,dV + \frac{N^2}{V^2}\,d\big(k_{\rm B}T\,B_2(T)\big) + \ldots \quad . \tag{6.51}$$

Dividing by dT, we find

$$T\left(\frac{\partial V}{\partial T}\right)_p - V = N\left[T\,\frac{\partial B_2}{\partial T} - B_2\right] \quad . \tag{6.52}$$

The temperature where $\big(\frac{\partial T}{\partial p}\big)_H$ changes sign is called the *inversion temperature* T^*. To find the inversion point, we set $T^*\,B_2'(T^*) = B_2(T^*)$, *i.e.*

$$\left.\frac{d\log B_2}{d\log T}\right|_{T^*} = 1 \quad . \tag{6.53}$$

If we approximate $B_2(T) \approx A - \frac{B}{T}$, then the inversion temperature follows simply:

$$\frac{B}{T^*} = A - \frac{B}{T^*} \qquad \Longrightarrow \qquad T^* = \frac{2B}{A} \quad . \tag{6.54}$$

6.3 Coulomb Systems : Plasmas and the Electron Gas

6.3.1 Electrostatic potential

Coulomb systems are particularly interesting in statistical mechanics because of their long-ranged forces, which result in the phenomenon of *screening*. Long-ranged forces wreak havoc with the Mayer cluster expansion, since the Mayer function is no longer integrable. Thus, the virial expansion fails, and new techniques need to be applied to reveal the physics of plasmas.

The potential energy of a Coulomb system is

$$U = \tfrac{1}{2}\int d^d\!r \int d^d\!r'\, \rho(\boldsymbol{r})\, u(\boldsymbol{r}-\boldsymbol{r}')\, \rho(\boldsymbol{r}') \quad , \tag{6.55}$$

where $\rho(\boldsymbol{r})$ is the charge density and $u(\boldsymbol{r})$, which has the dimensions of (energy)/(charge)^2, satisfies

$$\nabla^2 u(\boldsymbol{r}-\boldsymbol{r}') = -4\pi\, \delta(\boldsymbol{r}-\boldsymbol{r}') \quad . \tag{6.56}$$

Thus,

$$u(\boldsymbol{r}) = \begin{cases} -2\pi\, |x-x'| & , \quad d=1 \\ -2\,\log|\boldsymbol{r}-\boldsymbol{r}'| & , \quad d=2 \\ |\boldsymbol{r}-\boldsymbol{r}'|^{-1} & , \quad d=3 \quad . \end{cases} \tag{6.57}$$

For discete particles, the charge density $\rho(\boldsymbol{r})$ is given by

$$\rho(\boldsymbol{r}) = \sum_i q_i\, \delta(\boldsymbol{r}-\boldsymbol{x}_i) \quad , \tag{6.58}$$

where q_i is the charge of the i^{th} particle. We will assume two types of charges: $q=\pm e$, with $e>0$. The electric potential is

$$\phi(\boldsymbol{r}) = \int d^d\!r'\, u(\boldsymbol{r}-\boldsymbol{r}')\, \rho(\boldsymbol{r}') = \sum_i q_i\, u(\boldsymbol{r}-\boldsymbol{x}_i) \quad . \tag{6.59}$$

This satisfies the Poisson equation, $\nabla^2\phi(\boldsymbol{r}) = -4\pi\rho(\boldsymbol{r})$. The total potential energy can be written as

$$U = \tfrac{1}{2}\int d^d\!r\, \phi(\boldsymbol{r})\, \rho(\boldsymbol{r}) = \tfrac{1}{2}\sum_i q_i\, \phi(\boldsymbol{x}_i) \quad , \tag{6.60}$$

where it is understood that we omit self-interaction terms.

6.3.2 Debye-Hückel theory

We now write the grand partition function:

$$\begin{aligned} \Xi(T,V,\mu_+,\mu_-) = \sum_{N_+=0}^{\infty}\sum_{N_-=0}^{\infty} & \frac{1}{N_+!}\, e^{\beta\mu_+ N_+}\, \lambda_+^{-N_+ d} \cdot \frac{1}{N_-!}\, e^{\beta\mu_- N_-}\, \lambda_-^{-N_- d} \\ & \cdot \int d^d\!r_1 \cdots \int d^d\!r_{N_{\text{tot}}}\, e^{-\beta U(\boldsymbol{r}_1,\ldots,\boldsymbol{r}_{N_{\text{tot}}})} \quad , \end{aligned} \tag{6.61}$$

where $N_{\rm tot} = N_+ + N_-$. We adopt a *mean field* approach, known as *Debye-Hückel theory*, writing

$$\rho(\boldsymbol{r}) = \bar{\rho}(\boldsymbol{r}) + \delta\rho(\boldsymbol{r}) \qquad , \qquad \phi(\boldsymbol{r}) = \bar{\phi}(\boldsymbol{r}) + \delta\phi(\boldsymbol{r}) \quad . \tag{6.62}$$

We then have

$$\begin{aligned} U &= \tfrac{1}{2}\!\int\! d^d\!r \, \big[\bar{\rho}(\boldsymbol{r}) + \delta\rho(\boldsymbol{r})\big] \cdot \big[\bar{\phi}(\boldsymbol{r}) + \delta\phi(\boldsymbol{r})\big] \\ &= \tfrac{1}{2}\!\int\! d^d\!r \, \bar{\phi}(\boldsymbol{r})\, \bar{\rho}(\boldsymbol{r}) + \overbrace{\tfrac{1}{2}\!\int\! d^d\!r \, \bar{\phi}(\boldsymbol{r})\, \delta\rho(\boldsymbol{r}) + \tfrac{1}{2}\!\int\! d^d\!r \, \bar{\rho}(\boldsymbol{r})\, \delta\phi(\boldsymbol{r})}^{\text{these two terms are the same}} + \tfrac{1}{2}\!\int\! d^d\!r \, \delta\rho(\boldsymbol{r})\, \delta\phi(\boldsymbol{r}) \\ &= -\!\int\! d^d\!r \, \bar{\phi}(\boldsymbol{r})\, \bar{\rho}(\boldsymbol{r}) + \int\! d^d\!r \, \bar{\phi}(\boldsymbol{r})\, \rho(\boldsymbol{r}) + \overbrace{\tfrac{1}{2}\!\int\! d^d\!r \, \delta\rho(\boldsymbol{r})\, \delta\phi(\boldsymbol{r})}^{\text{ignore fluctuation term}} \\ &= -U_0 + \int\! d^d\!r \, \bar{\phi}(\boldsymbol{r})\, \rho(\boldsymbol{r}) + (\text{flucts})^2 \quad , \end{aligned} \tag{6.63}$$

where $U_0 \equiv \frac{1}{2}\!\int\! d^d\!r \, \bar{\phi}(\boldsymbol{r})\, \bar{\rho}(\boldsymbol{r})$, and we where have used $\delta\rho = \rho - \bar{\rho}$. Thus we have

$$\Xi = e^{U_0/k_{\rm B}T} \exp\!\bigg(z_+ \lambda_+^{-d} \!\int\! d^d\!r_+ \, e^{-e\,\bar{\phi}(\boldsymbol{r}_+)/k_{\rm B}T} \bigg) \exp\!\bigg(z_- \lambda_-^{-d} \!\int\! d^d\!r_- \, e^{e\,\bar{\phi}(\boldsymbol{r}_-)/k_{\rm B}T} \bigg) \tag{6.64}$$

whence

$$\Omega(T,V,\mu_+,\mu_-) = -U_0 - k_{\rm B}T z_+ \lambda_+^{-d} \!\int\! d^d\!r \, \exp\!\bigg(-\frac{e\,\bar{\phi}(\boldsymbol{r})}{k_{\rm B}T} \bigg) - k_{\rm B}T z_- \lambda_-^{-d} \!\int\! d^d\!r \, \exp\!\bigg(+\frac{e\,\bar{\phi}(\boldsymbol{r})}{k_{\rm B}T} \bigg) \quad , \tag{6.65}$$

where

$$\lambda_\pm = \bigg(\frac{2\pi\hbar^2}{m_\pm k_{\rm B}T} \bigg) \qquad , \qquad z_\pm = \exp\!\bigg(\frac{\mu_\pm}{k_{\rm B}T} \bigg) \quad . \tag{6.66}$$

Note that since $\bar{\phi}(\boldsymbol{r}) = \int\! d^d\!r' \, u(\boldsymbol{r} - \boldsymbol{r}')\, \bar{\rho}(\boldsymbol{r}')$ is a linear functional of $\bar{\rho}(\boldsymbol{r})$, we have

$$\frac{\delta U_0}{\delta\bar{\phi}(\boldsymbol{r})} = \bar{\rho}(\boldsymbol{r}) \quad . \tag{6.67}$$

We next demand that the free energy Ω is extremized with respect to the mean field $\bar{\phi}(\boldsymbol{r})$, *viz.*

$$0 = \frac{\delta\Omega}{\delta\bar{\phi}(\boldsymbol{r})} = -\bar{\rho}(\boldsymbol{r}) + e\,\lambda_+^{-d}\, z_+ \, \exp\!\bigg(-\frac{e\,\bar{\phi}(\boldsymbol{r})}{k_{\rm B}T} \bigg) - e\,\lambda_-^{-d}\, z_- \, \exp\!\bigg(+\frac{e\,\bar{\phi}(\boldsymbol{r})}{k_{\rm B}T} \bigg) \quad . \tag{6.68}$$

At $r \to \infty$, we assume charge neutrality and $\phi(\infty) = 0$. Thus

$$\lambda_+^{-d}\, z_+ = n_+(\infty) = \lambda_-^{-d}\, z_- = n_-(\infty) \equiv n_\infty \quad , \tag{6.69}$$

where n_∞ is the ionic density of either species at infinity. Therefore,

$$\rho(\boldsymbol{r}) = -2e\, n_\infty \sinh\!\bigg(\frac{e\,\phi(\boldsymbol{r})}{k_{\rm B}T} \bigg) \quad , \tag{6.70}$$

where we have dropped the bars on $\bar{\phi}$ and $\bar{\rho}$ for convenience. We now invoke Poisson's equation,

$$\nabla^2\phi = 8\pi e n_\infty \sinh(\beta e\phi) - 4\pi\rho_{\text{ext}} \quad , \tag{6.71}$$

where ρ_{ext} is an externally imposed charge density.

If $e\phi \ll k_{\text{B}}T$, we can expand the $\sinh$ function and obtain

$$\nabla^2\phi = \kappa_{\text{D}}^2\,\phi - 4\pi\rho_{\text{ext}} \quad , \tag{6.72}$$

where

$$\kappa_{\text{D}} = \bigg(\frac{8\pi n_\infty e^2}{k_{\text{B}}T}\bigg)^{1/2} \qquad , \qquad \lambda_{\text{D}} = \bigg(\frac{k_{\text{B}}T}{8\pi n_\infty e^2}\bigg)^{1/2} \quad . \tag{6.73}$$

The quantity λ_{D} is known as the *Debye screening length*. Consider, for example, a point charge Q located at the origin. We then solve Poisson's equation in the weak field limit,

$$\nabla^2\phi = \kappa_{\text{D}}^2\,\phi - 4\pi Q\,\delta(\boldsymbol{r}) \quad . \tag{6.74}$$

Fourier transforming, we obtain

$$-\boldsymbol{q}^2\,\hat{\phi}(\boldsymbol{q}) = \kappa_{\text{D}}^2\,\hat{\phi}(\boldsymbol{q}) - 4\pi Q \qquad \Longrightarrow \qquad \hat{\phi}(\boldsymbol{q}) = \frac{4\pi Q}{\boldsymbol{q}^2 + \kappa_{\text{D}}^2} \quad . \tag{6.75}$$

Transforming back to real space, we obtain, in three dimensions, the Yukawa potential,

$$\phi(\boldsymbol{r}) = \int\!\frac{d^3\!q}{(2\pi)^3}\,\frac{4\pi Q\,e^{i\boldsymbol{q}\cdot\boldsymbol{r}}}{\boldsymbol{q}^2 + \kappa_{\text{D}}^2} = \frac{Q}{r}\,e^{-\kappa_{\text{D}} r} \quad . \tag{6.76}$$

This solution must break down sufficiently close to $r = 0$, since the assumption $e\phi(r) \ll k_{\text{B}}T$ is no longer valid there. However, for larger r, the Yukawa form is increasingly accurate.

For another example, consider an electrolyte held between two conducting plates, one at potential $\phi(x = 0) = 0$ and the other at potential $\phi(x = L) = V$, where $\hat{\boldsymbol{x}}$ is normal to the plane of the plates. Again assuming a weak field $e\phi \ll k_{\text{B}}T$, we solve $\nabla^2\phi = \kappa_{\text{D}}^2\,\phi$ and obtain

$$\phi(x) = A\,e^{\kappa_{\text{D}} x} + B\,e^{-\kappa_{\text{D}}\,x} \quad . \tag{6.77}$$

We fix the constants A and B by invoking the boundary conditions, which results in

$$\phi(x) = \frac{V\sinh(\kappa_{\text{D}} x)}{\sinh(\kappa_{\text{D}} L)} \quad . \tag{6.78}$$

Debye-Hückel theory is valid provided $n_\infty\,\lambda_{\text{D}}^3 \gg 1$, so that the statistical assumption of many charges in a screening volume is justified.

6.3.3 The electron gas : Thomas-Fermi screening

Assuming $k_{\rm B}T \ll \varepsilon_{\rm F}$, thermal fluctuations are unimportant and we may assume $T = 0$. In the same spirit as the Debye-Hückel approach, we assume a slowly varying mean electrostatic potential $\phi(\boldsymbol{r})$. Locally, we can write

$$\varepsilon_{\rm F} = \frac{\hbar^2 k_{\rm F}^2}{2m} - e\phi(\boldsymbol{r}) \quad . \tag{6.79}$$

Thus, the Fermi wavevector $k_{\rm F}$ is spatially varying, according to the relation

$$k_{\rm F}(\boldsymbol{r}) = \bigg[\frac{2m}{\hbar^2}\Big(\varepsilon_{\rm F} + e\phi(\boldsymbol{r})\Big)\bigg]^{1/2} \quad . \tag{6.80}$$

The local electron number density is

$$n(\boldsymbol{r}) = \frac{k_{\rm F}^3(\boldsymbol{r})}{3\pi^2} = n_\infty \bigg(1 + \frac{e\phi(\boldsymbol{r})}{\varepsilon_{\rm F}}\bigg)^{3/2} \quad . \tag{6.81}$$

In the presence of a uniform compensating positive background charge $\rho_+ = en_\infty$, Poisson's equation takes the form

$$\nabla^2\phi = 4\pi e\, n_\infty \Bigg[\bigg(1 + \frac{e\phi(\boldsymbol{r})}{\varepsilon_{\rm F}}\bigg)^{3/2} - 1\Bigg] - 4\pi\rho_{\rm ext}(\boldsymbol{r}) \quad . \tag{6.82}$$

If $e\phi \ll \varepsilon_{\rm F}$, we may expand in powers of the ratio, obtaining

$$\nabla^2\phi = \frac{6\pi n_\infty e^2}{\varepsilon_{\rm F}}\,\phi \equiv \kappa_{\rm TF}^2\,\phi - 4\pi\rho_{\rm ext}(\boldsymbol{r}) \quad . \tag{6.83}$$

Here, $\kappa_{\rm TF}$ is the *Thomas-Fermi wavevector*,

$$\kappa_{\rm TF} = \bigg(\frac{6\pi n_\infty e^2}{\varepsilon_{\rm F}}\bigg)^{1/2} \quad . \tag{6.84}$$

Thomas-Fermi theory is valid provided $n_\infty\, \lambda_{\rm TF}^3 \gg 1$, where $\lambda_{\rm TF} = \kappa_{\rm TF}^{-1}$, so that the statistical assumption of many electrons in a screening volume is justified.

One important application of Thomas-Fermi screening is to the theory of metals. In a metal, the outer, valence electrons of each atom are stripped away from the positively charged ionic core and enter into itinerant, plane-wave-like states. These states disperse with some $\varepsilon(\boldsymbol{k})$ function (that is periodic in the Brillouin zone, *i.e.* under $\boldsymbol{k} \to \boldsymbol{k} + \boldsymbol{G}$, where $\boldsymbol{G}$ is a reciprocal lattice vector), and at $T = 0$ this *energy band* is filled up to the Fermi level $\varepsilon_{\rm F}$, as Fermi statistics dictates. (In some cases, there may be several bands at the Fermi level, as we saw in the case of yttrium.) The set of ionic cores then acts as a neutralizing positive background. In a perfect crystal, the ionic cores are distributed periodically, and the positive background is approximately uniform. A charged impurity in a metal, such as a zinc atom in a copper matrix, has a different nuclear charge and a different valency than the host. The charge of the ionic core, when valence electrons are stripped away, differs from that of the host ions, and therefore the impurity acts as a *local charge impurity*. For example, copper has an electronic configuration of $[\mathrm{Ar}]\,3d^{10}\,4s^1$. The $4s$ electron forms an energy band which contains the Fermi surface. Zinc has a configuration of

[Ar] $3d^{10}\,4s^2$, and in a Cu matrix the Zn gives up its two $4s$ electrons into the $4s$ conduction band, leaving behind a charge $+2$ ionic core. The Cu cores have charge $+1$ since each copper atom contributed only one $4s$ electron to the conduction band. The conduction band electrons neutralize the uniform positive background of the Cu ion cores. What is left is an extra $Q = +e$ nuclear charge at the Zn site, and one extra $4s$ conduction band electron. The $Q = +e$ impurity is, however, *screened* by the electrons, and at distances greater than an atomic radius the potential that a given electron sees due to the Zn core is of the Yukawa form,

$$\phi(\boldsymbol{r}) = \frac{Q}{r}\, e^{-\kappa_{\rm TF} r} \quad . \tag{6.85}$$

We should take care, however, that the dispersion $\varepsilon(\boldsymbol{k})$ for the conduction band in a metal is not necessarily of the free electron form $\varepsilon(\boldsymbol{k}) = \hbar^2\boldsymbol{k}^2/2m$. To linear order in the potential, however, the change in the local electronic density is

$$\delta n(\boldsymbol{r}) = e\phi(\boldsymbol{r})\, g(\varepsilon_{\rm F}) \quad , \tag{6.86}$$

where $g(\varepsilon_{\rm F})$ is the density of states at the Fermi energy. Thus, in a metal, we should write

$$\nabla^2\phi = (-4\pi)(-e\,\delta n) = 4\pi e^2 g(\varepsilon_{\rm F})\,\phi = \kappa^2_{\rm TF}\,\phi \quad , \tag{6.87}$$

where

$$\kappa_{\rm TF} = \sqrt{4\pi e^2\, g(\varepsilon_{\rm F})} \quad . \tag{6.88}$$

The value of $g(\varepsilon_{\rm F})$ will depend on the form of the dispersion. For ballistic bands with an effective mass m^*, the formula in eqn. 6.83 still applies.

The Thomas-Fermi atom

Consider an ion formed of a nucleus of charge $+Ze$ and an electron cloud of charge $-Ne$. The net ionic charge is then $(Z - N)e$. Since we will be interested in atomic scales, we can no longer assume a weak field limit and we must retain the full nonlinear screening theory, for which

$$\nabla^2\phi(\boldsymbol{r}) = 4\pi e \cdot \frac{(2m)^{3/2}}{3\pi^2\hbar^3}\Big(\varepsilon_{\rm F} + e\phi(\boldsymbol{r})\Big)^{3/2} - 4\pi Ze\,\delta(\boldsymbol{r}) \quad . \tag{6.89}$$

We assume an isotropic solution. It is then convenient to define

$$\varepsilon_{\rm F} + e\phi(\boldsymbol{r}) = \frac{Ze^2}{r}\cdot\chi(r/r_0) \quad , \tag{6.90}$$

where r_0 is yet to be determined. As $r \to 0$ we expect $\chi \to 1$ since the nuclear charge is then unscreened. We then have

$$\nabla^2\bigg\{\frac{Ze^2}{r}\cdot\chi(r/r_0)\bigg\} = \frac{1}{r_0^2}\,\frac{Ze^2}{r}\,\chi''(r/r_0) \quad , \tag{6.91}$$

thus we arrive at the *Thomas-Fermi equation*,

$$\chi''(t) = \frac{1}{\sqrt{t}}\,\chi^{3/2}(t) \quad , \tag{6.92}$$

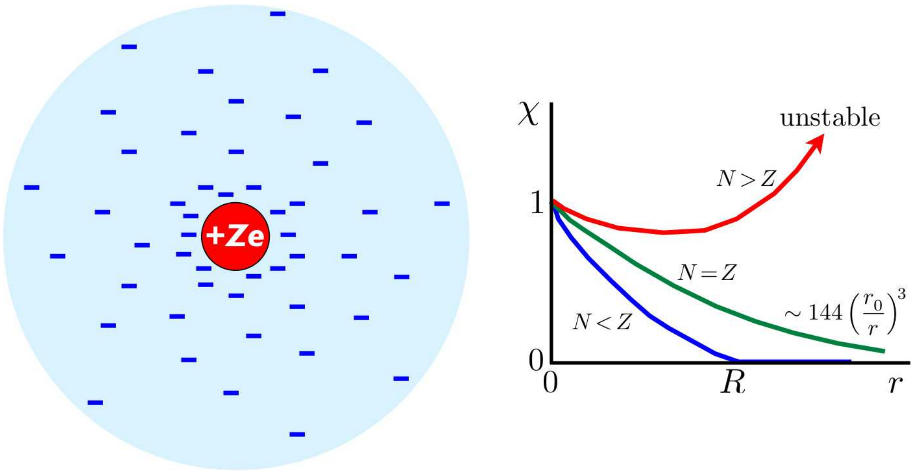

Figure 6.8: The Thomas-Fermi atom consists of a nuclear charge $+Ze$ surrounded by N electrons distributed in a cloud. The electric potential $\phi(\boldsymbol{r})$ felt by any electron at position $\boldsymbol{r}$ is screened by the electrons within this radius, resulting in a self-consistent potential $\phi(\boldsymbol{r}) = \phi_0 + (Ze^2/r)\,\chi(r/r_0)$.

with $r = t\,r_0$, provided we take

$$r_0 = \frac{\hbar^2}{2me^2}\left(\frac{3\pi}{4\sqrt{Z}}\right)^{2/3} = 0.885\,Z^{-1/3}\,a_{\mathrm{B}} \quad , \tag{6.93}$$

where $a_{\mathrm{B}} = \hbar^2/me^2 = 0.529\,\text{Å}$ is the Bohr radius. The TF equation is subject to the following boundary conditions:

- At short distances, the nucleus is unscreened, *i.e.* $\chi(0) = 1$.
- For positive ions, with $N < Z$, there is perfect screening at the ionic boundary $R = t^*\,r_0$, where $\chi(t^*) = 0$. This requires

$$\boldsymbol{E} = -\boldsymbol{\nabla}\phi = \left[-\frac{Ze^2}{R^2}\,\chi(R/r_0) + \frac{Ze^2}{R\,r_0}\,\chi'(R/r_0)\right]\hat{\boldsymbol{r}} = \frac{(Z-N)\,e}{R^2}\,\hat{\boldsymbol{r}} \quad . \tag{6.94}$$

This requires

$$-t^*\,\chi'(t^*) = 1 - \frac{N}{Z} \quad . \tag{6.95}$$

For an atom, with $N = Z$, the asymptotic solution to the TF equation is a power law, and by inspection is found to be $\chi(t) \sim C\,t^{-3}$, where C is a constant. The constant follows from the TF equation, which yields $12\,C = C^{3/2}$, hence $C = 144$. Thus, a neutral TF atom has a density with a power law tail, with $\rho \sim r^{-6}$. TF ions with $N > Z$ are unstable.